Title
7Li and 31P Magic Angle Spinning Nuclear Magnetic Resonance of LiFePO4-type materials

Journal
Electrochemical and Solid State Letters, 5(5)

Author
Cairns, Elton J.

Publication Date
2001-11-30

^{7}Li and ^{31}P MAS NMR of $LiFePO_4$-Type Materials

Michael C. Tucker[a], Marca M. Doeff[b], Thomas J. Richardson[a], Rita Fiñones[b], Jeffrey A. Reimer[a], and Elton J. Cairns[a]

a) Energy and Environmental Technologies Division

b) Materials Sciences Division

Ernest Orlando Lawerence Berkeley National Laboratory

and

Department of Chemical Engineering, University of California, Berkeley

Berkeley, CA 94720

Mailing Address:

Michael Tucker

UC Berkeley Chemical Engineering

201G Gilman Hall

Berkeley, CA 94720

Phone (510) 643-3073

FAX (510 642-4778

Email mctucker@uclink4.berkeley.edu

Abstract

$LiFePO_4$ and $LiMnPO_4$ have been characterized using ^{7}Li and ^{31}P MAS NMR spectroscopy. $LiFePO_4$ was synthesized by a hydrothermal route and $LiMnPO_4$ was synthesized at high temperature in an inert atmosphere. Both compositions give rise to single isotropic ^{7}Li resonances. The MAS isotropic peak linewidth for $LiFePO_4$ is considerably larger than that for $LiMnPO_4$, suggesting the presence of local disorder in the Li coordination sphere for $LiFePO_4$. In both samples, the isotropic peak is accompanied by a large, asymmetric spinning sideband manifold, arising from bulk magnetic susceptibility broadening and the paramagnetic interaction between the lithium nucleus and transition metal unpaired electrons.

Introduction

Much recent research has been focused on the possibility of using $LiFePO_4$ as a positive electrode material in lithium rechargeable batteries, especially those intended for transportation applications. Since the first reports of reversible lithium de-intercalation from $LiFePO_4$,[1,2] several research groups have developed methods of enhancing the electrochemical behavior of this material. Improvements have included coating the $LiFePO_4$ particles with a conductive carbonaceous layer to enhance the utilization,[3,4] preparing the materials at low temperature to preclude the formation of oxidized Fe^{3+} impurities,[5] and replacing some of the Fe with Mn to increase the operating voltage at the beginning of discharge.[6] Fundamental studies of $LiFePO_4$-related materials, however, have been limited; a few research groups have used Mössbauer spectroscopy[6,7] and EXAFS[8] to determine structural features pertaining to the Fe/Mn site. Magic angle spinning nuclear magnetic resonance (MAS NMR) spectroscopy is a complementary technique that is very sensitive to the atomic and electronic environment at the lithium site; successful application of the MAS NMR technique would allow direct observation of bulk Li in these interesting materials. NMR studies of electrode materials are, however, often obfuscated by effects of electronic, ionic, and magnetic properties of these materials. These effects can even preclude quantitative study without the use of specialized NMR techniques. We describe in this paper the direct observation of ^{7}Li and ^{31}P MAS NMR in the end members of the $Li(Fe,Mn)PO_4$ series, $LiFePO_4$ and $LiMnPO_4$.

Experimental Techniques

A modification of the hydrothermal method described by Whittingham et al.[9] was used to synthesize $LiFePO_4$. A mixture of $FeSO_4 \cdot 7H_2O$, H_3PO_4, and LiOH (mole ratios 1:1:3) dissolved in water were heated together at 120 ºC in a Teflon-lined Parr reactor for 24 hours. The resultant greenish-white powder was washed well with distilled water and dried overnight at 40 ºC in air. $LiMnPO_4$ was prepared from a 1:1 mixture of LiH_2PO_4 and $MnCO_3$ at 750°C in flowing N_2 for 16 hours. The sample contained a few percent of $Mn_2P_2O_7$.

Electrodes for lithium polymer cells were fabricated as previously described.[10] $Li/P(EO)_8LiTFSI/LiFePO_4$ cells were assembled and heated to 85 ºC for at least one hour prior to electrochemical testing. A MacPile II (Bio-Logic, SA, Claix, France) was used to cycle cells galvanostatically.

NMR experiments were performed on a Bruker AMX spectrometer, with a 7mm MAS probe (Doty Scientific) tuned to ^7Li frequency of 38.9MHz or ^{31}P frequency of 40.5MHz. ^7Li shifts were referenced to 1M $LiCl_{(aq)}$, and ^{31}P shifts were referenced to 85%H_3PO_4. A 90°-τ-180° (90°=1.2μs) pulse sequence with τ=(spinning frequency)$^{-1}$ was used to obtain the spectra shown. Recycle delays of 50ms and 20s were used to avoid saturation of the ^7Li and ^{31}P signals, respectively. Isotropic peaks were identified by varying the spinning speed. An inversion recovery sequence was used to measure T_1 (spin-lattice relaxation time). The spin-spin relaxation time (T_2) was estimated by varying the delay between the 90° and 180° pulses to be integer multiples of the rotor period.

Fitting the exponential decay of the echo intensity vs. pulse delay length yields an estimate of T_2.

Results and Discussion

The olivine $LiFePO_4$ structure contains electrochemically active Li in a framework composed of PO_4 tetrahedra and distorted FeO_6 octahedra. The strong covalent PO_4 unit tends to reduce the covalency of the Fe-O bond, modifying the redox potential for the $Fe^{2+/3+}$ couple, and thus producing a useful open-circuit potential for lithium extraction and reinsertion[1] (as shown in Figure 1). Mn can replace the Fe in the structure, although $LiMnPO_4$ is electrochemically inactive towards lithium extraction.[1] The local Li environment for $LiFePO_4$ is shown in Figure 2. The lattice positions were taken from the refinement of neutron diffraction, as presented in Reference 11. It is clear from Figure 2 that we might expect through-space or through-bond (specifically, the Li-O-Fe bond) transfer of unpaired electron density from the transition metal d-orbitals (Fe^{2+}:$t_{2g}^4e_g^2$ and Mn^{2+}:$t_{2g}^3e_g^2$) to the lithium orbitals, which could result in a significant NMR chemical shift for the ^{7}Li nucleus. The possibility of a Knight shift is unlikely in these materials because they are electronically insulating.

The ^{7}Li MAS NMR spectra of $LiFePO_4$ and $LiMnPO_4$ are shown in Figure 3. Both compositions give rise to a single isotropic ^{7}Li resonance, confirming the existence of a single lithium site in both structures. The isotropic ^{7}Li peak arising from the $LiFePO_4$ sample is considerably broader than that observed for the $LiMnPO_4$ sample. This large linewidth probably arises from chemical shift dispersion, suggesting that there is considerable local disorder in the coordination sphere of Li in $LiFePO_4$, perhaps in the

form of site vacancies or Li/Fe site mixing. The spin-lattice (T_1) and spin-spin (T_2) relaxation times were measured for both samples, and are presented in Table 1. The short T_1 times are typical of nuclei in paramagnetic materials because the coupling of nuclei to unpaired electrons is a very efficient relaxation mechanism. This fast relaxation allows the use of short NMR recycle delays and acquisition of high-quality spectra in a short period of time. The T_2 times measured for these materials are also quite short (more than 3 times shorter than those observed for ^{7}Li in $LiMn_2O_4$,[12] for example). We therefore expect considerable dephasing and loss of echo intensity during the MAS rotor period, suggesting that faster spinning speeds would be desirable.

A large manifold of spinning sidebands accompanies the isotropic ^{7}Li MAS NMR peaks for both compositions studied here. Linebroadening which can be reduced to a spinning sideband pattern under MAS can result from quadrupolar interaction of the nucleus with a local electric field gradient, nuclear dipolar coupling (to ^{7}Li or ^{31}P), paramagnetic coupling (to localized, unpaired transition metal electrons), chemical shift anisotropy (CSA) or bulk magnetic susceptibility effects. A significant contribution from the quadrupolar interaction is unlikely: we would not expect an appreciable electric field gradient at the Li site because of the local near-octahedral symmetry. No distinct quadrupolar satellites were observed. Furthermore, nutation data were consistent with excitation of all the ^{7}Li spin states: 90° pulse lengths measured for the $LiMPO_4$ samples were identical to that measured for 1M LiCl in water (1.2μs), whereas the 90° pulse would have been half as long if only the central transition was being excited (and not the quadrupolar satellites). The nuclear dipolar contribution is largely averaged away by magic angle spinning. The ^{7}Li isotropic peak linewidth for $LiMnPO_4$, however, decreased

slightly with increasing spinning speed, suggesting that some residual dipolar broadening is present in these materials.[13] The effect of spinning speed was probably masked by the large residual linewidth in the $LiFePO_4$ sample.

We are left, then, with CSA, paramagnetic coupling, and bulk magnetic susceptibility effects as the remaining possible contributors to the large spinning sideband manifold. It is clear in Figure 3 that there is a large asymmetry in the sideband manifold observed for $LiMnPO_4$ (and to a lesser extent $LiFePO_4$). It is therefore tempting to assign the broadening to CSA. However, the local near-octahedral symmetry of the Li site would seem to preclude a significant CSA contribution to the sideband manifold. We therefore assert that the large sideband manifold arises not from CSA, but from anisotropic paramagnetic coupling and bulk magnetic susceptibility. This assertion is supported by a comparison of ^{7}Li and ^{31}P MAS NMR spectra, below.

In the $LiMPO_4$ structure the PO_4 unit displays strong covalent bonds[1] and is very nearly tetrahedral, precluding any significant CSA interaction for the ^{31}P nucleus. On the basis of this information, we expect a single, featureless ^{31}P resonance, such as that observed for K_3PO_4 (Figure 4a), possibly accompanied by a sideband manifold arising from paramagnetic coupling and bulk magnetic susceptibility. The ^{31}P NMR spectrum of $LiMnPO_4$ (Figure 4b) yields an isotropic ^{31}P peak at -10ppm, consistent with a partial oxygen bridging to the Li or Fe site.[14,15] The spectrum also shows a broad sideband manifold, with nearly identical asymmetry to that observed for ^{7}Li in $LiMnPO_4$, implying that the asymmetry arises from the same fundamental mechanism. The similarity is made apparent in the comparison of spectra shown in Figure 4b. The sideband manifolds for ^{7}Li and ^{31}P NMR of $LiFePO_4$ were also coincident (not shown). CSA is unlikely to give

rise to such similar sideband patterns from different nuclei in different chemical sites. The absence of CSA is consistent with the negligible ^{7}Li quadrupolar effects discussed above; assuming the chemical shift is dominated by electronic effects, we would expect anisotropy in the chemical shift to be accompanied by significant quadrupolar broadening. We therefore conclude that the broad, asymmetric sideband manifold for $LiMPO_4$ materials arises from anisotropic paramagnetic coupling and bulk magnetic susceptibility. It is not surprising to find anisotropy in these interactions, given the non-cubic magnetic lattice for these materials, shown in Figure 5.

Asymmetric sideband envelopes have been interpreted previously to yield structural information pertaining to the distribution of paramagnetic centers in solid compounds.[16,17] Such studies are most successful when the bulk magnetic susceptibility arising from the localized paramagnetic centers is small and isotropic. In the present compounds, the bulk magnetic susceptibility is expected to be large, due to the high concentration of paramagnetic centers, and probably contains an anisotropic part due to the non-cubic transition metal lattice (Figure 5). The anisotropic part of the bulk magnetic susceptibility (ABMS) is expected to be manifest as an increase in the residual MAS linewidth for the individual sidebands.[18-20] The above discussion of the residual linewidth would suggest that such ABMS broadening is not a significant contributor to the observed linewidth for $LiMnPO_4$, although a contribution to that observed for $LiFePO_4$ cannot be ruled out on the basis of the present data.

The large isotropic part of the susceptibility is expected to give rise to inhomogeneous linebroadening that can be "spun away" with MAS, but nevertheless contributes to the shape of the sideband manifold. It would therefore be desirable to

remove the effects of the bulk magnetic susceptibility before attempting to quantify the structural information contained in the asymmetry of the sideband manifold. The "susceptibility matching" technique for minimizing bulk magnetic susceptibility effects has been described previously,[21,22] and involves immersion of the sample powder in a solution which has the same bulk magnetic susceptibility as the solid particles. The magnetic boundaries of the sample are then determined by the sample holder, and not the individual powder particles. We attempted to match the susceptibility of the $LiMPO_4$ samples with a saturated aqueous solution of $Er(NO_3)_3$.[22] No change in the shape of the NMR spectrum was observed, probably because the bulk susceptibility of the sample powders was too high to be effectively matched. The following analysis was therefore performed on the unmatched spectra.

We estimated the anisotropic shift and asymmetry parameter that describe the paramagnetic coupling using *HBA*, a widely available program for applying Herzfeld-Berger analysis[23] to MAS spectra. The anisotropic shift, δ, and the asymmetry parameter, η, are defined as

$$\delta=\delta_{33}-\delta_{iso} \quad (1a)$$

$$\eta=(\delta_{22}-\delta_{11})/\delta \quad (1b)$$

where δ_{iso} is the isotropic chemical shift and δ_{11}, δ_{22}, and δ_{33} are the principal components of the paramagnetic interaction tensor. δ represents the linewidth of the paramagnetic broadening, while η indicates the deviation of the interaction symmetry from the extremes of axial symmetry (η=0) or spherical symmetry (η=1). This analysis does not account for the effects of susceptibility broadening, which masks the paramagnetic anisotropy. The calculated values are presented in Table 1. It should be noted that this

analysis can also be used to describe CSA, although CSA and paramagnetic broadening arise from different mechanisms.

Conclusions

We have studied $LiFePO_4$ and $LiMnPO_4$ using MAS NMR spectroscopy. Both compositions give rise to single isotropic ^7Li resonances, accompanied by broad spinning sideband manifolds. The ^7Li isotropic MAS peak linewidth for $LiFePO_4$ is probably dominated by chemical shift dispersion, suggesting some disorder in the local Li coordination sphere. The MAS linewidth for $LiMnPO_4$ contains a significant contribution from residual dipolar broadening. The spinning sideband manifold is notably asymmetric in the case of $LiMnPO_4$, and slightly asymmetric in the case of $LiFePO_4$. Comparing the sideband manifolds for ^7Li and ^{31}P MAS NMR spectra of the samples confirmed that the sideband manifold arises primarily from anisotropic paramagnetic coupling and bulk magnetic susceptibility broadening. Future work will focus on determining the shift mechanism which gives rise to the positive and negative ^7Li NMR shifts observed in these materials.

Acknowledgements

This work was supported by the Assistant Secretary for Energy Efficiency and Renewable Energy, Office of Transportation Technologies of the U.S. Department of Energy under Contract No. DE-AC03-76SF00098.

References

1. Padhi, A.K., K.S. Nanjundaswamy, and J.B. Goodenough, *J. Electrochem. Soc.*, **144**(4), 1188-1194 (1997).
2. Padhi, A.K., K.S. Nanjundaswamy, C. Masquelier, S. Okada, and J.B. Goodenough, *J. Electrochem. Soc.*, **144**(5), 1609-1613 (1997).
3. Ravet, N., Y. Chouinard, J.F. Magnan, S. Besner, M. Gauthier, and M. Armand, *J. Power Sources*, **97-98**, 503-507 (2001).
4. Prosini, P.P., D. Zane, and M. Pasquali, *Electrochim. Acta*, **46**, 3517-3523 (2001).
5. Yang, S., P.Y. Zavalij, and M.S. Wittingham, *Electrochem. Comm.*, **3**, 505-508 (2001).
6. Yamada, A. and S.-C. Chung, *J. Electrochem. Soc.*, **148**(8), A960-A967 (2001).
7. Andersson, A.S., B. Kalska, L. Haggstrom, and J.O. Thomas, *Solid State Ionics*, **130**, 41-52 (2000).
8. S. Yang, P. Y. Zavalij, and M. S. Whittingham, *Electrochem. Commun.*, **3**, 505 (2001).
9. M. M. Doeff, M. Y. Peng, Y. Ma, and L.C. De Jonghe, *J. Electrochem. Soc.*, **141**, L145 (1994).
10. Yamada, A., Y. Kudo, and K.-Y. Liu, *J. Electrochem. Soc.*, **148**(10), A1153-A1158 (2001).
11. Andersson, A.S. and J.O. Thomas, *J. Power Sources*, **97-98**, 498-502 (2001).

12. Tucker, M.C., J.A. Reimer, and E.J. Cairns, *J. Electrochem. Soc.*, **148**(8), A951-A959 (2001).

13. Popov, A.I. and K. Hallenga, *Modern NMR Techniques and their Application in Chemistry*. Practical Spectroscopy, ed. E.G. Brame. Vol. 11., Marcel Dekker, Inc., New York (1991).

14. Fayon, F., D. Massiot, K. Suzuya, and D.L. Price, *J. Non-Cryst. Sol.*, **283**, 88-94 (2001).

15. Cody, G.D., B. Mysen, G. Saghi-Szabo, and J.A. Tossell, *Geochim. Cosmochim. Acta*, **65**(14), 2395-2411 (2001).

16. Nayeem, A, and J.P. Yesinowski, *J. Chem. Phys.*, **89** (8), 4600 (1988).

17. Brough, A.R., C.P. Grey, and C. M. Dobson, *J. Am. Chem. Soc.*, **115**, 7318 (1993).

18. Alla, M. and E. Lippmaa, *Chem. Phys. Lett.*, **87**(1), 30 (1982).

19. VanderHart, D.L., W.L. Earl, and A.N. Garroway, *J. Magn. Reson.*, **44**, 361 (1981).

20. Kubo, A., T.P. Spaniol, and T. Terao, *J. Magn. Reson.*, **133**, 330 (1998).

21. Stoll, M.E. and T.J. Majors, *J. Magn. Reson.*, **46**, 283 (1982).

22. Grey, C.P., C. M. Dobson, and A.K. Cheetham, *J. Magn. Reson.*, **98**, 414 (1992).

23. Herzfeld, J. and A.E. Berger, *J. Chem. Phys.*, **73**, 6021 (1980).

List of Tables

List of Figures

Table 1.

Sample	$\delta_{isotropic}$ (ppm)	T_1 (ms)	T_2(ms)	δ (ppm)	η
$LiFePO_4$	-14	1.2	440	1360	0.97
$LiMnPO_4$	63	3.9	220	1380	0.83

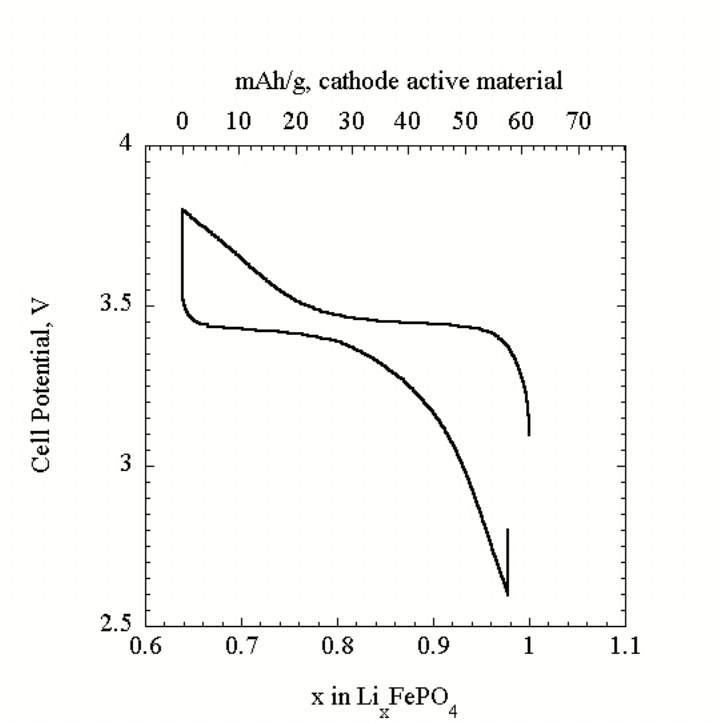
mAh/g, cathode active material
0
10
20
30
40
50
60
70
4
3.5
3
2.5
Cell Potential, V
0.6
0.7
0.8
0.9
1
1.1
x in Li$_x$FePO$_4$

Figure 1.

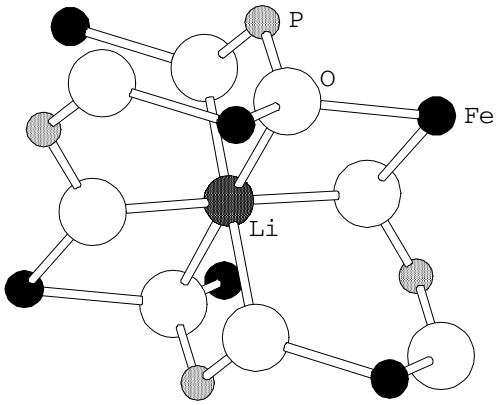

Figure 2.

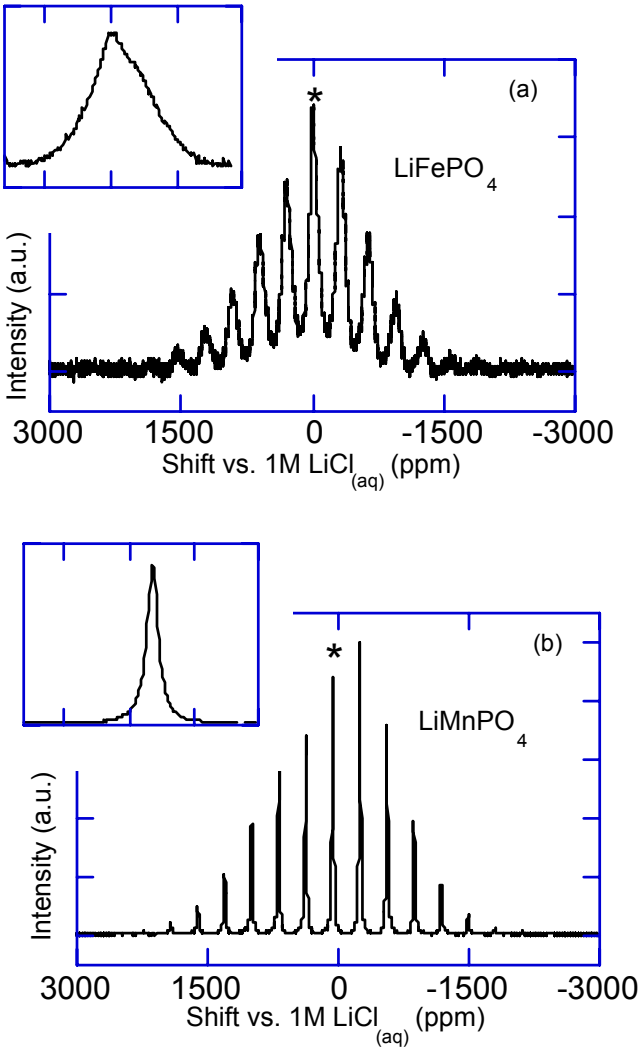
(a)
*
LiFePO4
Intensity (a.u.)
3000
1500
0
-1500
-3000
Shift vs. 1M LiCl(aq) (ppm)
(b)
*
LiMnPO4
Intensity (a.u.)
3000
1500
0
-1500
-3000
Shift vs. 1M LiCl(aq) (ppm)

Figure 3.

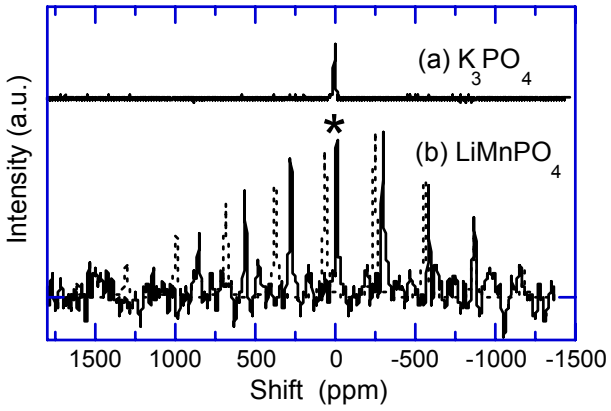
(a) K3PO4
(b) LiMnPO4
*
Intensity (a.u.)
1500
1000
500
0
-500
-1000
-1500
Shift (ppm)

Figure 4.

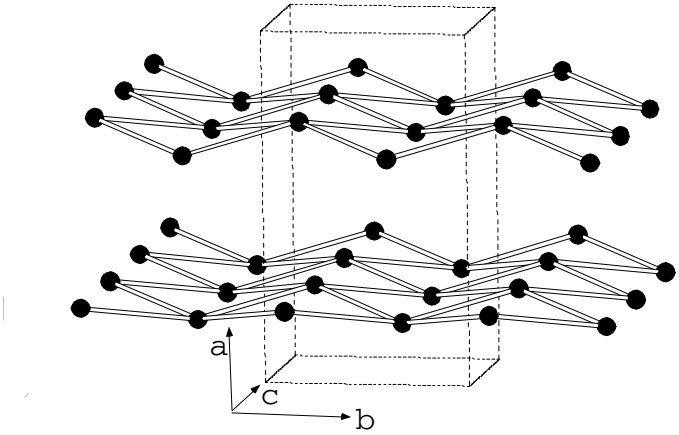

Figure 5.